ISSN 1392-2114 ULTRAGARSAS, Nr.3(33). 1999.

Measurements of electromechanical coupling coefficient for surface acoustic waves in proton-exchanged lithium niobate

D. Čiplys, R. Rimeika

Vilnius University, Laboratory of Physical Acoustics

Faculty of Physics, Saulėtekio 9, 2040 Vilnius, LITHUANIA,

Phone: +370 2 33 60 34, E-mail: daumantas.ciplys@ ff.vu.lt

Introduction

Proton-exchanged (PE) lithium niobate ($LiNbO_3$) integrated optical waveguides have attracted considerable attention because of their relatively simple fabrication technique and the high refractive index changes obtained [1]. Since the interaction of surface acoustic waves (SAWs) with guided optical modes offers important applications in the field of communications and data processing [2], the investigations of SAW propagation in PE $LiNbO_3$ crystals deserve great interest. The SAW propagation in pure lithium niobate is well studied since this material is one of the most widely used in acoustic applications [3]. The proton exchange leads to substantial changes in the crystal structure and material properties, affecting, therefore, the SAW propagation characteristics. The partial substitution of lithium ions by protons results in formation, at the crystal surface, of a $H_xLi_{1-x}NbO_3$ layer which may exist in different phases. Up to seven different phases have been reported [4]. It is the formation of surface layer that is responsible for changes in the acoustic wave propagation characteristics caused by the proton exchange. The surface acoustic wave velocity perturbation by the proton exchange was first observed by [5]. A large decrease in the velocity (up to 20 % at the frequency 180 MHz) has been found for the *X*-propagation on *Y*- and *Z*-cut surfaces. The SAW velocity in PE $LiNbO_3$ has been studied using Brillouin scattering technique at acoustic frequencies of order 10 GHz in *Y*-cut samples [6], with the help of the acoustic microscope at 215 MHz on *X*, *Y* and *Z* cuts [7], by the acoustoptic diffraction method at 180 MHz and 420 MHz in *Y*-cut samples [8], and from the frequency response of SAW interdigital transducer at about 80 MHz in *Z*-cut substrates [9]. The detailed studies of dispersion characteristics of the SAW in the frequency range from 100 MHz up to over 1 GHz in *Y*-cut crystals and evaluation of elastic stiffness constants of the $H_xLi_{1-x}NbO_3$ layer have been performed in [10]. The SAW velocities in *Z*-cut crystals with different $H_xLi_{1-x}NbO_3$ phases have been studied by the acoustooptic diffraction technique in a wide frequency range 60-400 MHz [11].

It should be noted that the performance of proton exchange in $LiNbO_3$ is sensitive to the crystal orientation. A very strong surface damage by the PE in *Y*-cut crystals has been reported [12] making this orientation disadvantageous for applications. Most oftenly, the *Z*-cut crystals are used for PE studies and optical waveguides applications. However, the electromechanical coupling coefficient K^2 which is an important parameter determining the efficiency of surface acoustic wave excitation and detection is relatively low for this cut even in pure lithium niobate. Therefore, the interest naturally arises in using a crystal orientation which would match virtues of the higher electromechanical coupling coefficient value and absence of the surface damage. Such is the 128° rotated *Y*-cut $LiNbO_3$ substrate, widely known in the acoustic field. The interaction of surface acoustic waves and guided optical modes in PE 128° rotated *Y*-cut $LiNbO_3$ has been first demonstrated in [13] at acoustic frequency 130 MHz. The SAW propagation in PE samples of this cut has been studied by measuring the interdigital transducer response near 100 MHz [14] and by the acoustooptic diffraction technique in a frequency range 30-600 MHz [15].

As the factor of primary importance for many SAW devices is the electromechanical coupling coefficient, it is important to know its behaviour in lithium niobate subjected to the proton exchange. For *YZ* configuration, it has been shown [16] that the exchange reduces significantly the K^2 implying that the $H_xLi_{1-x}NbO_3$ layer possess no piezoelectric effect. This assumption was used by authors of Ref.10 when evaluating the elastic properties of the protonated layer. Concerning the other cuts, some contradictory results have been obtained. For the *Z*-cut, a noncomplete reduction of piezoelectric activity in the layer has been reported [9] , though one might be confused that authors reported the value of K^2 for pure (nonexchanged) crystal which was twice as large as the commonly reported values. Similarly, for 128° rot. *Y*-cut substrate, the piezoelectric effect in a protonated layer has been reported to be reduced but not completely vanish [14]. In [16], the change in the electromechanical coupling coefficient has been evaluated from the increase in acoustic transmission losses between two interdigital transducers, and in [9,14] the K^2 values were determined by measuring the radiation impedance of an interdigital transducer at resonance frequency. Here we present another approach for measuring the electromechanical coupling coefficient in proton-exchanged lithium niobate: the method is based on measuring *in situ* the SAW attenuation during slow evaporation of a metal film on the wave propagation path [17].

Definition of electromechanical coupling coefficient

Some basic relations necessary for further considerations are given below in this chapter. More detailed analysis can be found elsewhere (e.g. in [18]).

The propagation of acoustic waves in an anisotropic elastic medium possessing the piezoelectric properties is described by four coupled differential equations

$$\rho \frac{\partial^2 u_j}{\partial t^2} - c_{ijkl} \frac{\partial^2 u_k}{\partial x_i \partial x_l} - e_{kij} \frac{\partial^2 \varphi}{\partial x_k \partial x_i} = 0, \quad (1)$$

$$e_{ikl} \frac{\partial^2 u_k}{\partial x_i \partial x_l} - \varepsilon_{ik} \frac{\partial^2 \varphi}{\partial x_i \partial x_k} = 0, \quad i,j,k,l = 1,2,3 \quad (2)$$

Consider the plane bulk wave propagating in the unlimited medium of the form

$$u_i = \alpha_i \exp ik(b_i x_i - Vt) \quad (3)$$

$$\varphi = \alpha_4 \exp ik(b_i x_i - Vt) \quad (4)$$

where V is the phase velocity, k is the wavenumber , and the propagation direction is determined by the unit vector $\boldsymbol{b}$ in the coordinate system x_i. The amplitude of potential φ can be expressed through the amplitudes of mechanical displacement $\boldsymbol{u}$ with the help of Eq. 2 as

$$\alpha_4 = \alpha_j \frac{e_{ijk} b_i b_k}{\varepsilon_{pq} b_p b_q} \quad . \quad (5)$$

Substituting (5) into (1) one obtains

$$\rho V^2 \alpha_j = c'_{ijkl} b_i b_i \alpha_k \quad (6)$$

where

$$c'_{ijkl} = c_{ijkl}\left(1 + K^2_{ijkl}\right) \quad (7)$$

and

$$K^2_{ijkl} \equiv \frac{e_{mij} e_{nkl} b_m b_n}{c_{ijkl}\left(\varepsilon_{pq} b_p b_q\right)} \quad (8)$$

is the electromechanical coupling coefficient. One can see from Eqs. 6 to 8 that the influence of the piezoelectric effect can be accounted for by increasing the elastic constants by the factor $(1+K^2_{ijkl})$. It is said that the piezoelectricity "stiffens" the crystal lattice.

Solution of Eq. 6 yields the bulk wave velocity for a given propagation direction and polarisation in the form

$$V' = \left(c'/\rho\right)^{1/2} \quad (9)$$

where c' is the appropriate linear combination of stiffened elastic coefficients. As the value of electromechanical coupling coefficient is much less than unity, one may write

$$V' = V\left(1 + K^2/2\right) \quad (10)$$

where $V \equiv \left(c/\rho\right)^{1/2}$ is the acoustic velocity in the absence of the piezoelectric effect, and K^2 is the electromechanical coupling coefficient for given orientation.

In the case of surface acoustic waves the Eqs. 6 to 8 can not be applied. The surface waves are essentially nonhomogenous, and the relation between the amplitudes of mechanical displacement $\boldsymbol{u}$ and potential φ becomes dependent on the distance from the surface.

The electromechanical coupling coefficient for surface acoustic waves is then defined by the analogy with Eq. 10 as

$$\frac{K^2}{2} = \frac{V_f - V_m}{V_f} \quad (11)$$

where V_f is the SAW velocity on a free surface of the piezoelectric, and V_m is the SAW velocity on a surface covered with an infinitely thin perfectly conducting layer. The idea for such a definition is that the conductivity layer shortens the tangential component of the electric field created by the wave due to the piezoelectric effect reducing the contribution of the latter. The parameter thus defined is of great importance as it serves as a quantitative characteristic of piezoelectric materials with respect to surface acoustic waves. The values of K^2 in lithium niobate have been calculated for various crystal cuts and SAW propagation directions [19,20]. For orientations along the crystallographic axes, as well for the practically important rotated cut, the results of calculations are shown in Table 1.

Table 1. **Electromechanical coupling coefficients for surface acoustic waves in $LiNbO_3$ for various cuts and propagation directions**

Crystal cut	SAW propagation direction	Free surface velocity, m/s	Metallized surface velocity, m/s	Electro-mechanical coupling coefficient , 10^{-2}
X	Y	3748	3681	3.58
X	Z	3483	3396	5.00
Y	X	3769	3740	1.54
Y	Z	3488	3404	4.82
Z	X	3798	3788	0.53
Z	Y	3903	3859	2.25
128° rot Y	X	3994	3888	5.31

Such a definition of the electromechanical coupling coefficient may be employed for characterization not only of simple semi-space substrates but also of more complex layered structures. It is the purpose of present paper to study the electromechanical coupling coefficient in lithium niobate substrates subjected to the proton exchange procedure which changes considerably the properties of a crystal layer near the surface.

Proton exchange process

The proton exchange process in lithium niobate serves as a technique enabling to form good quality optical waveguiding layers in a crystal with an objective of integrated optics applications. The method was first employed by [1], and since that deserved numerous studies and applications. The proton exchange is a process in which the lithium ions of the crystal lattice are partially substituted by hydrogen ions (protons) supplied from an ambient medium. Usuallly the proton exchange in lithium niobate is performed by keeping the samples in benzoic acid (C_6H_5COOH) at temperatures about 200°C for times from several minutes to several hours. The rate of exchange may be controlled by diluting a small amount of lithium benzoate ($C_7H_5LiO_2$). Other types of acids like phosphoric (H_3PO_4), pyrophosphoric ($H_4P_2O_7$), adipic ($HOOC(CH_2)_4COOH$) and other (see e.g. [4]) proton sources are also used.

As a result, a layer of $H_xLi_{1-x}NbO_3$ is formed at the sample surface with crystal structure and physical properties differing from those of $LiNbO_3$. It is the

property of enhanced extraordinary refractive index in the layer due to which the propagation of guided optical modes becomes possible.

The distribution of protons in the crystal may be substantially affected by the post-exchange annealing [21]. The latter procedure reduces the number of defects introduced by the exchange process and is used to ameliorate the temporal stability of the guides formed. The annealing is usually performed at temperatures of several hundreds centigrade degrees, mostly in air, for very different time periods (from several minutes to several hours).

Measurements of SAW attenuation during metal evaporation

The method chosen is based on *in situ* measurements of the SAW attenuation during the evaporation of a metal film on the substrate surface [22,23]. This technique enables, in addition, to evaluate the dielectric permittivity of the substrate "seen" by the acoustic wave [24]. The scheme of experiment is shown in Fig. 1. The samples prepared for measurements had middle parts subjected to the proton exchange. The interdigital transducers for SAW excitation and detection were deposited in the nonexchanged regions, and the strip electrodes for film resistance measurements were deposited at the sides of exchanged area. A sample was then covered with a mask having a rectangular window in the middle through which copper was thermally evaporated at a rate less than 1 nm/s onto the surface area between the strip electrodes. The rf pulses of duration about 1 μs were fed into the input transducer to excite the SAW and the variation in the pulse amplitude U_{out} at the output transducer was monitored during evaporation. The attenuation of SAW in dB per length unity was determined as

$$A = \frac{1}{W} 20\lg \frac{U_{\text{in}}}{U_{\text{out}}} \tag{12}$$

where U_{in} is the pulse amplitude at the output transducer in the absence of the metal film, W is the length of metallised region in the SAW propagation direction. The resistance of the film during evaporation was measured as the ratio of dc current I and voltage U, and the film sheet resistivity (resistance of a square area) of the film was determined as

$$R_{\text{s}} = \frac{U}{I}\frac{W}{L} \tag{13}$$

where L is the distance between dc electrodes.

According to the theory of interaction between a SAW propagating on a piezoelectric substrate and free charge carriers in an adjacent thin conductive film [25]. The attenuation arising due to the creation of alternating currents in the film by piezoelectric fields of the SAW can be expressed as

$$A = 4.34K^2_{eff}\frac{\omega}{V}\frac{\omega_{\text{C}}/\omega}{1+(\omega_{\text{C}}/\omega)^2} \tag{14}$$

where $\omega = 2\pi f$ is the angular frequency and V is the velocity of the SAW, and the dielectric relaxation frequency is defined as

$$\omega_{\text{c}} = \frac{\omega}{\varepsilon_{\text{o}}\varepsilon_{eff} V R_{\text{S}}} \tag{15}$$

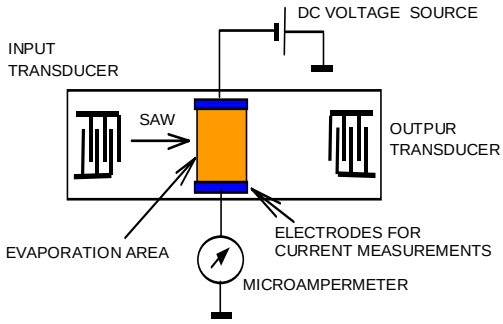

Fig. 1**. Schematic diagram of SAW attenuation vs evaporated film resistance measurements.**

where ε_0 is the dielectric permittivity of free space. The subscript "eff" emphasizes that electromechanical coupling coefficient K^2_{eff} and the relative dielectric permittivity ε_{eff} are effective parameters of the structure "seen" by the surface acoustic wave and depend both on $LiNbO_3$ substrate and $H_xLi_{1-x}NbO_3$ layer properties. It may be omitted below. The maximum attenuation occurs when $\omega_{\text{c}} = \omega$ or at sheet resistivity

$$R_{\text{S}} = \frac{1}{\varepsilon_0 \varepsilon_{\text{eff}} V} \tag{16}$$

The maximum attenuation value is

$$A_{\max} = 2.17K^2_{\text{eff}}\frac{2\pi f}{V} \tag{17}$$

The effective electromechanical coefficient is evaluated from the experimentally measured value of attenuation maximum using (17) , and the effective dielectric permittivity is found from the position of maximum in the R_S scale using (16). The SAW velocities, necessary for calculations, have been measured using the acousto-optic diffraction technique [15]. For each sample and frequency value, the K^2 evaluation experiment has been repeated for several times. As the evaluated values varied within an interval up to 10 % , the values of K^2 are the averaged ones.

Effect of evaporated area length

In order to check the validity of the method, we performed the evaluation of the electromechanical coupling coefficient for pure (nonexchanged) *Y*-cut *Z*-propagation and 128° rotated Y-cut *X*-propagation lithium niobate crystals, the coupling coefficient values for which are well known. The measurements of SAW attenuation during metal evaporation were carried out at different frequencies and evaporated area lengths *W*. The results are shown in Table 2. Our experiments revealed the variations in attenuation per unit length measured for the same frequency but different evaporated area lengths.

Such an effect is not predicted by the theoretical considerations given above and may be attributed to an increased influence of the boundaries between free and metallized surface regions when the evaporated area dimensions become comparable to the acoustic wavelength. This can be clearly seen from Fig. 2 where the attenuation normalized to the acoustic frequency is plotted as a function of the evaporated area length and SAW wavelength ratio. With decreasing W/λ ratio, the decrease

in A/f values is observed, and these values cannot be used for the K^2 evaluation. In order to obtain the correct values of electromechanical coupling coefficient, the length of evaporated area must be at least as large as five times the acoustic wavelength. This requirement was satisfied in the measurements described below.

Table 2. **Attenuation values measured in pure crystals for different frequencies and evaporated area lengths.**

Orientation	f, MHz	W, mm	A, dB/mm
YZ	28	0.12	4.03
	57	0.12	9
	57	0.46	10.2
	57	1.37	10.2
	173	0.12	31.2
128° rot.*YX*	32	0.12	3.71
	32	0.25	4.38
	32	0.46	5.9
	32	1.37	5.84
	120	0.12	19.2
	120	0.46	22
	370	0.12	66.3

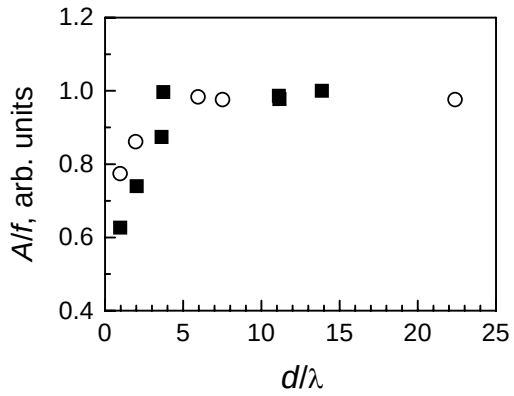

Fig. 2**. SAW attenuation normalized to frequency vs evaporated area length-acoustic wavelength ratio in nonexchanged lithium niobate. Crystal orientations: YZ (open circles), 128° rotated YX (solid squares).**

Results for PE 128° rotated Y-cut $LiNbO_3$

Here we present results, which are desribed more in details in [17]. In our experiments, we performed the proton exchange in pure benzoic acid. Some of the samples were annealed after the exchange. In order to evaluate the characteristics of the layers formed, guided optical waves have been excited and their effective refractive indices measured. From these, the refractive index profiles (depth dependences) in proton-exchanged samples have been reconstructed. The profiles in as-exchanged samples exhibit a step-like shape, and one is able to use in further considerations the model of simple layer-on-substrate structure with layer thickness directly determined from the profile. The refractive index profile experiences a considerable change due to the post-

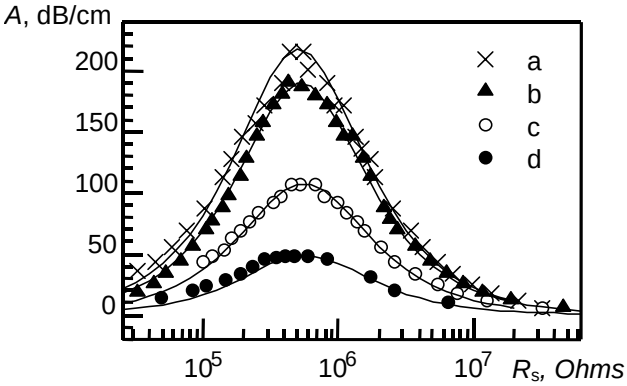

Fig. 3. **Change in SAW attenuation against sheet resistivity of Cu film during its evaporation. Dots are measured values in lithium niobate samples: non-exchanged (a), and proton-exchanged at 230°C for 1 (b) , 10 (c), 25 (d) hours. Solid curves are calculated from Eq. (15) with best-fit values of K^2.**

exchange annealing. The step is transformed to the graded distribution function as the initial amount of protons penetrates, due to diffusion, into deeper regions. The single layer approximation is not aplicable in this case. However , one may introduce an effective thickness in order to enable a comparison with step-like profile data. An effective thickness of a graded layer can be defined as a thickness of the step which has the same area as the graded function and the height equal to the function value at the very surface.

The dependences of SAW attenuation upon the sheet resistivity measured for several exchanged samples as well for the non-exchanged sample, are presented in Fig. 3. They are fitted to the curves calculated from Eq. 14. For non-exchanged lithium niobate we obtain $\varepsilon_{\text{eff}}=54\varepsilon_0$ and $K^2=0.053$ what is in a good agreement with data commonly used in the literature. No shift of the attenuation maximum in the R_S scale is observed for proton exchanged samples implying that the dielectric permittivity of the $H_xLi_{1-x}NbO_3$ layer remains close to that of the $LiNbO_3$ substrate. The attenuation value at its maximum considerably decreases with increasing the thickness of protonated layer or the SAW frequency. In Fig. 4, all the measured values of K^2

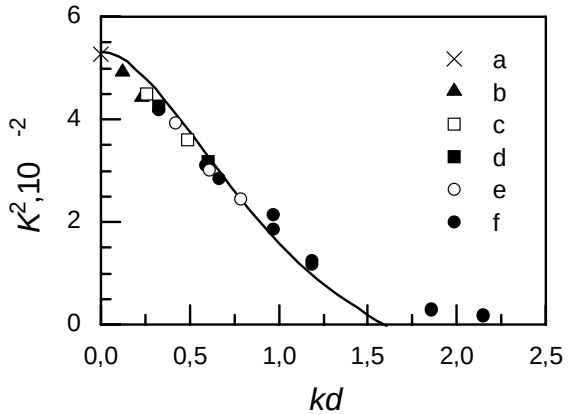

Fig. 4. **Electromechanical coupling coefficient in proton exchanged lithium niobate as function of acoustic wavenumber-layer thickness product. Dots are values obtained from SAW attenuation measurements during metal evaporation in non-exchanged sample (a) and samples exchanged at 230°C for: 1 (b), 5.5 (c), 6 (d), 10 (e), 25 (f) hours. Line depicts values obtained from SAW velocity measurements on free and metallised surface in sample (c).**

are plotted as a function of the normalized parameter *kd,* where $k=\omega/V$ is the acoustic wavenumber. The fact that all the experimental points lay on the same curve serves as evidence for validity of the single homogenous layer model used. With increasing *kd,* the electromechanical coupling coefficient tends to zero implying that piezoelectric fields created by the surface acoustic wave decay significantly within the $H_xLi_{1-x}NbO_3$ layer. This observation confirms the assumption that $H_xLi_{1-x}NbO_3$ is nonpiezoelectric. If the piezoelectric effect in the layer would exist (though reduced), the dependence would be saturated at non-zero K^2_{eff} value with growing *kd*. It should be noted that the maximum *kd* value attained by the authors [14] was only 0.7 where K^2 is really about 0.03, whereas for its reduction by the factor of order from the initial value, *kd* values twice as large are necessary.

The post-exchange annealing procedure which is frequently used in the PE optical waveguide technology has been reported to have a strong influence on the proton distribution in the crystal and the refractive index profile of the waveguide [21]. It may cause the changes in the lattice structure $H_xLi_{1-x}NbO_3$ layer as different phases of the latter may exist depending on the relative amount of protons *x* [26,27]. The question now arises what is the influence of post-exchange annealing on the electromechanical coupling coefficient in the structure. The sample which had been proton-exchanged at 230 °C for 25 h was subjected to consecutive annealings in air at temperatures 300, 360, 410, and 450°C, each of 1 h duration. The comparatively long time of the initial exchange was chosen in order to obtain the multi-mode optical waveguide whose profile could be reliably determined. As usually, the evolution from the step-like profile to the graded one due to the redistribution of protons with consecutive steps of annealing is observed. It should be noted that no guided mode propagation was observed after the fourth annealing step, possibly due to the formation of thin $LiNb_3O_8$ layer at the very surface of the crystal as suggested in [27].

The dependences of electromechanical coupling coefficient upon acoustic frequency are shown in Fig. 5. As the shape of the layer profile experiences significant transformations at various stages of treatment, the slight monotonous drop of the electromechanical coupling coefficient at given frequency is observed. This suggests that the layer formed at the surface by the proton exchange remains non-piezoelectric. It should be noted that partial restoring of the electromechanical coupling coefficient in *Y*-cut PE samples has been reported in [16].

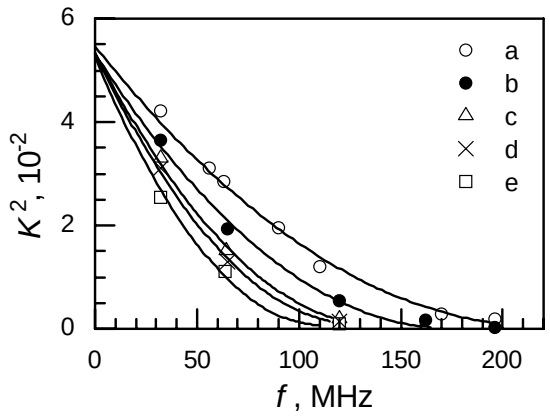

Fig. 5. **Influence of annealing on electromechanical coupling coefficient in proton-exchanged lithium niobate. Sample was proton-exchanged at 230°C for 25 h (a) and annealed for 1 h at 300 (b), 360 (c), 410 (d), 450 (e) °C**.

Results for PE Z-cut $LiNbO_3$

In contrast to previous observations, below we report on the increase of electromechanical coupling coefficient in lithium niobate subjected to proton exchange treatment. A more detailed description of the results reported here can be found in [28]. The experiments were carried out in *Z*-cut crystals with *X*-propagating surface acoustic waves. The samples were fabricated using various proton sources and treatment procedures in order to obtain different phases of $H_xLi_{1-x}NbO_3$ layers [29]. They are listed in Table 3.

The dependences of SAW attenuation upon the sheet resistivity of evaporated Cu film are shown in Fig.6 for proton-exchanged sample S1 as well as for nonexchanged sample S0. One can clearly see the difference in heights of the attenuation maxima. The experimental dependences are in a good agreement with the curves calculated from Eq.14 using ε and K^2 as fitting parameters. For the nonexchanged sample we obtain K^2 value $0.46\cdot10^{-2}$ which is close to value $0.53\cdot10^{-2}$ reported in [20] for pure $LiNbO_3$. The substantially enhanced value $0.85\cdot10^{-2}$ is obtained in the exchanged sample. The measurements of SAW attenuation maxima during Cu film evaporation have been performed for all the samples listed in Table 3, at various frequencies, and K^2 values have been calculated from Eq.17.

Table 3. **Values of squared electromechanical coupling coefficient K^2 measured for proton-exchanged *Z*-cut *X*-propagation $LiNbO_3$ at different frequencies *f* for samples characterized by different protonated layer thicknesses *d* and surface acoustic wave velocities *V*.**

Sample	*d*, μm	*f*, MHz	*V*, m/s	K^2, 10^{-2}
S0	-	94	3795	0.46
S1	1.85	31	3780	0.48
		93	3720	0.81
S2	2.85	75	3740	0.84
S3	2.14	93	3690	0.8
S4a	9.14	31	3700	0.71
		75	3665	0.37
		92	3613	0.29
S5	4.3	74	3626	0.7
		91	3570	0.65
		114	3541	0.47
S7	2.9	32	3780	0.53
		63	3760	0.67
		75	3747	0.83
		94	3735	0.81
		117	3725	0.7

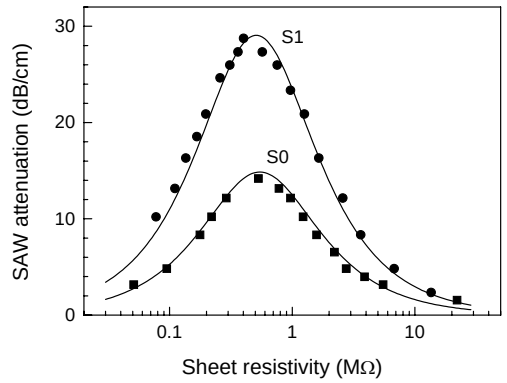

Fig.6. **Variation of SAW attenuation against sheet resistivity of the evaporated Cu film at 94 MHz in nonexchanged S0 and proton-exchanged S1 samples. Dots represent experimentally measured values, solid curves are calculated from Eq.(1) with K^2=0,44·10^{-2} and ε=55 for S0, and K^2 =0,85·10^{-2} and ε=60 for S1**.

In order to compare the results obtained for different samples, the evaluated values of squared electromechanical coupling coefficient are plotted in Fig.7 as a function of normalized parameter *kd*, where $k = 2\pi f / V$ is the acoustic wavenumber, and *d* is the protonated layer thickness defined as described above. It is interesting to note that the data obtained in different samples can be approximated by a single curve. The same values of electromechanical coupling coefficient are obtained in samples fabricated at different conditions provided the product *kd* is the same. The coupling coefficient grows with increasing *kd* up to about 0.4, that is in the range of acoustic wavelengths larger than the protonated layer thickness at least by the order of magnitude. Further increase in *kd* leads to reduction of K^2 with the tendency to attain zero. Such a reduction of the electromechanical coupling coefficient is consistent with the assumption of nonpiezoelectric layer over the piezoelectric substrate. Concerning the initial growth in K^2 value, it may be attributed to changes in the distribution of electrical potential of the SAW in the presence of $H_xLi_{1-x}NbO_3$ layer on *ZX*-$LiNbO_3$. This should be proved by numerical calculations of the potential distribution in our samples what is, however, out of the scope of the present paper.

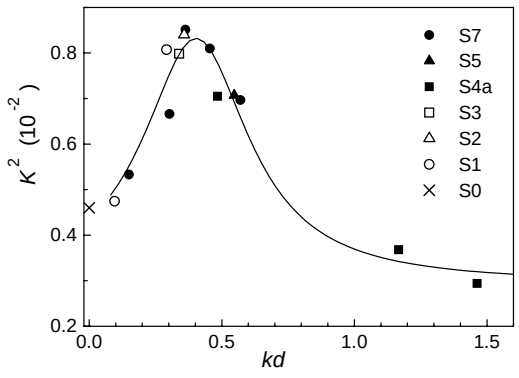

Fig.7**. Electromechanical coupling coefficient values measured in different samples against acoustic wavenumber-layer thickness product.**

Conclusions

The electromechanical coupling coefficient for surface acoustic waves in proton-exchanged 128° rotated Y-cut *X*-propagation and Z-cut X-propagation lithium niobate has been measured using the method of evaporation of a thin copper film on the SAW propagation path and measuring variations in the SAW attenuation. Due to the proton exchange, the electromechanical coupling coefficient in rotated Y-cut crystals is reduced as compared with that in a non-exchanged sample. The decrease in K^2 value depends on the acoustic frequency and protonated layer thickness: the greater is the *kd* product, the weaker is the coupling coefficient. The latter tends to zero at sufficiently high frequencies or thick layers, implying that the $H_xLi_{1-x}NbO_3$ layer possess no piezoelectric activity. The post-exchange annealing leads to a slight further decrease of electromechanical coupling coefficient indicating that the piezoelectric properties are not restored.

The enhancement in K^2 value due to the proton exchange procedure has been observed in Z-cut crystals. The electromechanical coupling coefficient appeared to depend on the acoustic wavelength- layer thickness product rather than on the sample history. The K^2 value attains maximum of about $0.8 \cdot 10^{-2}$ at $kd \approx 0.4$ whereas it is equal to $0.46 \cdot 10^{-2}$ in nonexchanged lithium niobate. The increase in electromechanical coupling coefficient can be applied for enhancement of the SAW interdigital transducer efficiency.

Acknowledgement

The authors would like to thank Yu.N.Korkishko and V.A. Fedorov for supplying *Z*-cut $LiNbO_3$ samples.

References

1. **Jackel J. L., Rice C. E., Veselka J. J**. Proton exchange for high-index waveguides in $LiNbO_3$ // Appl. Phys. Lett. -1982.-Vol. 41. P. 607–608.
2. **Tsai C.S.** Integrated acousto-optic circuits and applications // IEEE Trans. Ultrason. Ferroelectr. Freq. Control.-1992.-Vol. 39. P.529–554.
3. **Shimizu Y.** Current status of piezoelectric substrate and propagation characteristics for SAW devices // Jpn. J. Appl. Phys.- 1993.- Vol. 32. P.2183–2187.
4. **Korkishko Yu. N., Fedorov V. A., Kostrickii S. M**. Optical and x-ray characterization of $H_xLi_{1-x}NbO_3$ phases in proton-exchanged $LiNbO_3$ optical waveguides // J. Appl. Phys. -1998.- Vol. 84. P. 2411–2419.
5. **Hinkov V., Ise E**. Surface acoustic velocity perturbation in $LiNbO_3$ by proton exchange // J. Phys. D: Appl. Phys. -1985.- Vol. 18. P.L31-–L34.
6. **Hinkov V., Barth M., Dransfeld K.** Acoustic properties of proton exchanged $LiNbO_3$ investigated by Brillouin scattering // Appl. Phys A. -1985.-Vol. 38. P.269–273.
7. **Burnett P. J., Briggs G. A., Al-Shukri S. M., Duffy J. F., De La Rue R. M.** Acoustic properties of proton-exchanged $LiNbO_3$ studied using the acoustic microscopy $V(z)$ technique // J. Appl. Phys. –1986.- Vol. 60. P.2517–2522.
8. **Hinkov V.** Proton exchanged waveguides for surface acoustic waves in $LiNbO_3$ // J. Appl. Phys. –1987.- Vol. 62. P.3573–3578.
9. **Chen Y. C., Cheng C. C.** Proton-exchanged *Z*-cut $LiNbO_3$ waveguides for surface acoustic waves // IEEE Trans. Ultrason. Ferroelectr. Freq. Control. –1996.- Vol. 43. P.417–421.

10. **Biebl E. M., Russer P.** Elastic properties of proton exchanged lithium niobate // IEEE Trans. Ultrason. Ferroelectr. Freq. Control.- 1992.- Vol. 39. P.330–334.
11. **Čiplys D., Rimeika R., Korkishko Yu. N., Fedorov V. A.** Velocities of surface acoustic waves in proton exchanged lithium niobate with different $H_xLi_{1-x}NbO_3$ phases // Ultragarsas.-1998.- Vol. 29. P.24–28.
12. **Campari A., Ferrari C., Mazzi G., Summonte C., Al-Shukri S. M., Dawar A., De La Rue R. M., Nutt A. C. G.** Strain and surface damage induced by proton exchange in *Y*-cut $LiNbO_3$ // J. Appl. Phys. –1985.- Vol. 58. P.4521–4524.
13. **Saiga N., Ichioka Y.** Acousto-optic interaction in proton-exchange 128° rotated *Y*-cut $LiNbO_3$ optical waveguides // J. Appl. Phys. – 1987.- Vol. 61. P.1230–1233.
14. **Kakio S., Matsuoka J., Nakagawa Y.** Surface acoustic wave properties on proton-exchanged 128°-rotated *Y*-cut $LiNbO_3$ // Jpn. J. Appl. Phys., Part 1. –1993.- Vol. 32. P.2359–2361.
15. **Paškauskas J., Rimeika R., Čiplys D.** Velocity and attenuation of surface acoustic waves in proton-exchanged 128° rotated *Y*-cut $LiNbO_3$ // J. Phys. D: Appl. Phys. – 1995.- Vol. 28. P.1419–1423.
16. **Hickernell F. S., Ruehle K. D., Joseph S. J., Reese G. M., Weller J. F.** The surface acoustic wave properties of proton exchanged *YZ* lithium niobate // IEEE Ultrasonics Symposium Proceedings. –1985.- P.237–240.
17. **Čiplys D., Rimeika R.** Electromechanical coupling coefficient for surface acoustic waves in proton-exchanged 128°-rotated *Y*-cut lithium niobate // Appl. Phys.Lett. –1998.- Vol. 73. P.2417–2419.
18. **Auld B. A.** Acoustic fields and waves in solids // John Wiley and Sons, New York. –1973.
19. **Campbell J. J., Jones W. R.** A method for estimating optimal crystal cuts and propagation directions for excitation of piezoelectric surface waves // IEEE Trans. Son. Ultrason. –1968.- Vol.15. P.209–217.
20. **Slobodnik A. J., Conway E. D., Delmonico R.T.** Microwave Acoustics Handbook 1A // Air Force Cambridge Research Laboratories, Hanscom. –1973.
21. **De Micheli M., Botineau J., Neveu S., Sibillot P., Ostrowsky D.B., Papuchon M.** Independent control of index and profiles in proton-exchanged lithium niobate guides // Optics Letters. – 1983.- Vol. 8. P.114–115.
22. **Bierbaum P.** Interaction of ultrasonic surface waves with conduction electrons in thin metal films // Appl. Phys.Lett. –1972.-Vol. 21. P.595–598.
23. **Sereika A. P., Garška E. P., Milkevičiene Z. A., Jučys A.J.** Electronic attenuation of surface acoustic wave in piezoelectric-metal film structure // Solid State Physics (in Russian). –1974.- Vol. 16. P.2415–2417.
24. **Kotelianskii I. M., Krikunov A. I., Medved A. V., Miskinis R. A.** Measurement of effective electromechanical coupling constant and effective dielectric permittivity of piezoelectric- thin dielectric layer structures // Microelectronics (in Russian).- 1981.- Vol.10. P.543–545.
25. **Ingebrigtsen K. A.** Linear and non-linear attenuation of acoustic surface waves in a piezoelectric coated with a semiconducting film // J. Appl. Phys. –1970.- Vol. 41. P.454–459.
26. **Rice C. E.** The structure and properties of $Li_{1-x}H_xNbO_3$ // J. Solid State Chem. -1986.- Vol. 64. P.188–191.
27. **Ganshin V. A., Korkishko Yu. N.** H:$LiNbO_3$ waveguides: effects of annealing // Optics Comm. –1991.- Vol. 86. P.523–530.
28. **Čiplys D., Rimeika R., Korkishko Yu. N., Fedorov V.A.** Enhancement of electromechanical coupling coefficient by proton exchange in *z*-cut $LiNbO_3$ // Appl. Phys. Lett. –2000.- (in press).
29. **Korkishko Yu. N., Fedorov V. A., Kostritskii S. M.** Optical and x-ray characterization of $H_xLi_{1-x}NbO_3$ phases in proton-exchanged $LiNbO_3$ optical waveguides // J. Appl. Phys. –1998.- Vol. 84. P.2411-2419.

D. Čiplys, R. Rimeika

Elektromechaninio ryšio koeficiento paviršinėms akustinėms bangoms protonų pakaitos ličio niobate matavimai

Reziumė

Elektromechaninio ryšio koeficientas paviršinėms akustinėms bangoms (PAB) protonų pakaitos 128° pasukto Y pjūvio X sklidimo ir Z pjūvio X sklidimo ličio niobate eksperimentiškai tyrinėtas lėtai garinant metalinę plėvelę ir matuojant *in situ* PAB slopinimą. Nustatyta, kad garinamos srities ilgis PAB sklidimo kryptimi turi būti ne mažesnis kaip penki bangos ilgiai. Pasuktojo pjūvio kristaluose elektromechaninio ryšio koeficientas mažėja iki nulio, didinant protonuoto sluoksnio storį ar akustinės bangos dažnį. Tai rodo, kad, atlikus protonų pakaitą, pjezoelektrinis efektas paviršiniame kristalo sluoksnyje išnyksta. Z pjūvio kristaluose pastebėtas naujas reiškinys - elektromechaninio ryšio koeficiento padidėjimas dėl protonų pakaitos. Šis reiškinys aiškinamas akustinės bangos elektrinio potencialo persiskirstymu prie kristalo paviršiaus.

Pateikta spaudai 1999 12 15

DOI: 10.5755/j01.u.33.3.7945